*Proc. Natl. Acad. Sci. USA*
Vol. 83, pp. 3513–3517, May 1986
Neurobiology

# Low-dimensional chaos in an instance of epilepsy

(chaotic attractors/electroencephalogram/Lyapunov exponents/phase space)

A. BABLOYANTZ AND A. DESTEXHE

Faculte des sciences, Universite Libre de Bruxelles, Campus Plaine CP 231, Boulevard du Triomphe, 1050 Brussels, Belgium

*Communicated by I. Prigogine, December 23, 1985*

ABSTRACT **Using a time series obtained from the electroencephalogram recording of a human epileptic seizure, we show the existence of a chaotic attractor, the latter being the direct consequence of the deterministic nature of brain activity. This result is compared with other attractors seen in normal human brain dynamics. A sudden jump is observed between the dimensionalities of these brain attractors (4.05 ± 0.05 for deep sleep) and the very low dimensionality of the epileptic state (2.05 ± 0.09). The evaluation of the autocorrelation function and of the largest Lyapunov exponent allows us to sharpen further the main features of underlying dynamics. Possible implications in biological and medical research are briefly discussed.**

Recent progress in the theory of nonlinear dynamical systems has provided new methods for the study of time series in such fields as hydrodynamics (1), chemistry (2), climatic variability (3, 4), biochemistry (5, 6), and human brain activity (7). The study of such complex systems may be performed by analyzing experimental data recorded as a series of measurements in time of a pertinent and easily accessible variable of the system. In most cases, such variables describe a global or averaged property of the system. For example, a time series may be obtained by recording at regular time intervals the mean electrical activity of a portion of the mammalian cortex. Although it may seem that such data offer only a one-dimensional view of the activity of the brain, this is not the case: it can be shown that a time series may provide information about a large number of pertinent variables, which may subsequently be used to explore and characterize the system's dynamics (8).

More specifically, by using a time series one can determine the possibility of constructing an attractor and thereby establishing the deterministic character of the dynamics of the underlying system. This topological entity portrays the essential features of the system's dynamics and may be characterized by the numerical value of its Hausdorff dimension $D$. A steady state is represented by a point attractor $D = 0$ and a time periodic regime exhibits a line attractor with $D = 1$. In general, if $D$ is a noninteger—that is, a fractal dimension—we may be in the presence of a chaotic attractor. The main feature of chaotic attractors is their sensitivity to the initial conditions. After a lapse of time, it is increasingly difficult to predict the future evolution of the system from a given initial state.

In this paper, we analyze the electrical activity of the human cortex by means of the electroencephalogram (EEG) recorded from an epileptic human patient and also from normal persons during sleep cycles. First, on the basis of analyses of the time series of EEG data, we show the existence of an epileptic attractor and determine its correlation dimension $\nu$, which is easily accessible from experimental data. Then, we analyze other dynamical properties of the time series, such as Lyapunov exponents and time autocorrelation function. The next section analyzes EEG data recorded during various stages of the sleep cycle. In the final section, we discuss the relevance of the EEG analyses to the understanding of brain activity.

## Epileptic Attractor

Epileptic seizures reflect a pathological state of the brain activity, which may occur spontaneously as a result of functional disorders or lesions, or may be induced by various means. There are several forms of epilepsy (9); here we are concerned with seizures of short duration (≈5 sec) known as "petit mal." This type of generalized epilepsy may invade the entire cerebral cortex and shows a bilateral symmetry between the two hemispheres. During the seizure, the EEG activity suddenly switches into an apparently oscillating mode. A succession of more or less regular and extremely coherent waves of ≈3 cycles per sec may be seen. The waves are separated by less regular spikes. Fig. 1 shows four simultaneous recordings during a seizure. Channels 1 and 2 form the basis of our time series, which will be used for the construction of the phase space trajectories.

Let us assume that the dynamics of the brain activity is described by a set of $\{X_0(t), X_1(t), \ldots, X_{n-1}(t)\}$ variables satisfying a system of first-order differential equations. A differential equation of order $n$ with a single variable $X_0$, accessible from experimental data, is equivalent to the original set. Now both $X_0$ and its derivatives, therefore the ensemble of $n$ variables, can be obtained from a single time series. However, it is more convenient to construct another set of variables $\{X_0(t), X_0(t + \tau), \ldots, X_0[t + (n - 1)\tau]\}$, which is topologically equivalent to the original set (8) ($X_0$ may represent the electrical potential $V$ recorded by EEG). These variables are obtained by shifting the original time series by a fixed time lag $\tau$ ($\tau = m\Delta t$, where $m$ is an integer and $\Delta t$ is the interval between successive samplings).

These variables span a phase space, which allows the drawing of the phase portrait of the system or, more precisely, its projection into a low-dimensional subspace of the full phase space. If the dynamics are reducible to deterministic laws, the system reaches in time a state of permanent regime. This fact is reflected by the convergence of families of phase trajectories toward a subset of the phase space. This invariant subset is the attractor.

The phase space trajectories extracted from the time series of the seizure shown in Fig. 1 have been constructed in a three-dimensional phase space spanned by the variables $V(t)$, $V(t + \tau)$, and $V(t + 2\tau)$. Fig. 2 shows four views of the phase space portrait corresponding to four different rotations of the $V(t + \tau) - V(t + 2\tau)$ plane around the $V(t)$ axis. The phase portraits of Fig. 2 are constructed from channel 1 of Fig. 1 and are almost the same as those obtained from channel 2. These data have been recorded from both hemispheres and show a large spatial coherence of the phenomenon. This coherence also appears in a striking fashion in the phase portraits of Fig. 2. In the following two sections, we show that these phase trajecto-

The publication costs of this article were defrayed in part by page charge payment. This article must therefore be hereby marked "*advertisement*" in accordance with 18 U.S.C. §1734 solely to indicate this fact.

Abbreviation: EEG, electroencephalogram.

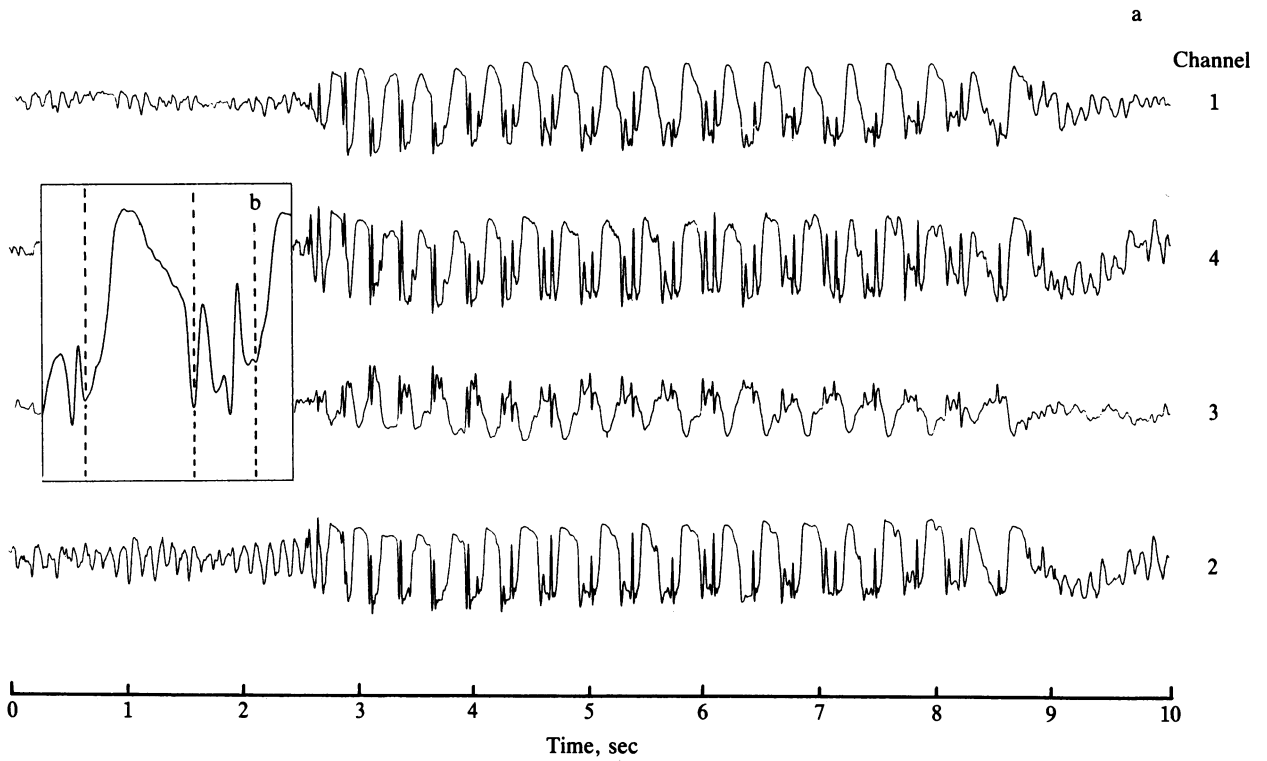


FIG. 1. (*a*) EEG recording of a human epileptic seizure of petit mal activity. Channel 1 (left) and channel 3 (right) measure the potential differences between frontal and parietal regions of the scalp, whereas channel 2 (left) and channel 4 (right) correspond to the measures between vertex and temporal regions. This seizure episode, lasting ≈5 sec, is the longest and the least noise-contaminated EEG selected from a 24-hr recording on a magnetic tape of a single patient. Digital PDP 11 equipment was used. The signal was filtered below 0.2 Hz and above 45 Hz and is sampled in 12 bits at 1200 Hz. (*b*) One pseudocycle is formed from a relaxation wave and spikes.

ries do indeed define a chaotic attractor of low dimension. Very similar results are obtained from channels 3 and 4. However, the attractors are slightly blurred since these channels are contaminated by muscular activity because of their position on the scalp.

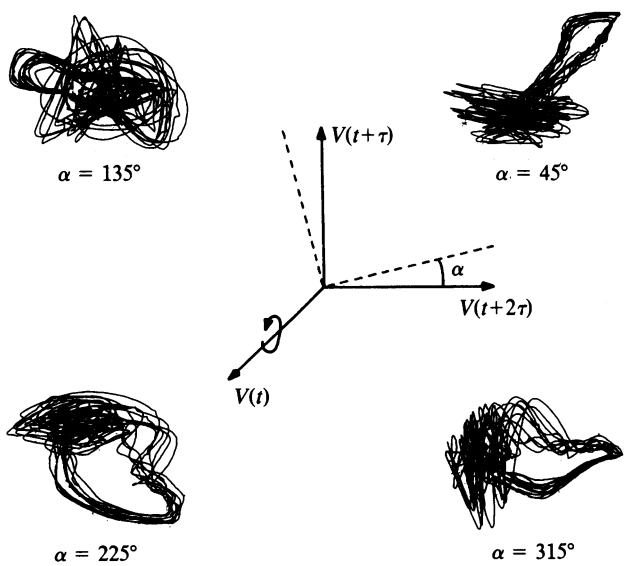


FIG. 2. Phase portraits of human epileptic seizure. First, the attractor is represented in a three-dimensional phase space. The figure shows two-dimensional projections after a rotation of an angle $\alpha$ around the $V(t)$ axis. The time series is constructed from the first channel of Fig. 1 ($n$ = 5000 equidistant points and $\tau$ = 19 $\Delta t$). Nearly identical phase portraits are found for all $\tau$ in the range from 17 $\Delta t$ to 25 $\Delta t$ and also in other instances of seizure.

In Fig. 3, we follow the unfolding in time of the phase trajectories during one pseudocycle as shown in the box of Fig. 1*b*. Fig. 3*b* shows the part of the trajectory covered by the brain dynamics during the wave-like activity, whereas Fig. 3*c* shows the part arising from the spikes. The direction of winding of the attractor is always the same, as shown by the arrows. Therefore, following Rössler, we can refer to the attractor as spiral or screw chaos (10).

From the inspection of Figs. 2 and 3, we infer that the part of the trajectories emanating from wave activity have a tendency to remain in a plane and behave like a noise-prone periodic motion. This plane is perpendicular to the bundle of trajectories corresponding to the spike activity, which introduces chaotic elements into the phase portrait, and this fact increases the dimension of the attractor.

## Topological Aspects of Epilepsy

Fractal objects such as chaotic attractors can be characterized by a Hausdorff dimension $D$. In general, the evaluation of the Hausdorff dimension is not easy; therefore, one introduces a

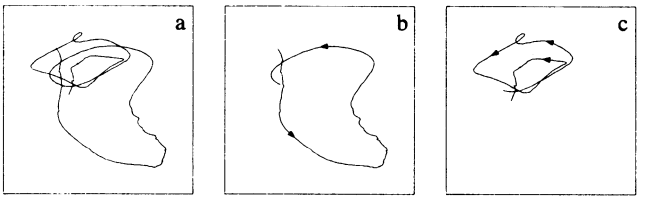


FIG. 3. Evolution of phase trajectories in time ($\tau$ = 19 $\Delta t$ and $\alpha$ = 225°). (*a*) Phase portraits of one pseudocycle. (*b*) Part of the trajectories emanating from the wave activity. (*c*) Contribution from spike activity. Arrows show the direction of rotation of the trajectories.

more accessible correlation dimension (11, 12) $\nu \leq D$, which may be obtained easily from numerical analysis of the time series in Fig. 1. Notice that if $p$ represents the embedding dimension of the attractor then, necessarily, $D \leq p$.

We introduce a vector notation: $\mathbf{V}_i(t)$ stands for a point of phase space whose coordinates are $\{V(t_i), V(t_i + \tau), \ldots, V[t_i + (n-1)\tau]\}$. A "reference" point $\mathbf{V}_i$ from these data is chosen and its distances $|\mathbf{V}_i - \mathbf{V}_j|$ from the $n-1$ remaining points are computed. This allows us to count the data points that are within a prescribed distance $r$ from the point $\mathbf{V}_i$ in the phase space. Repeating the process for all values of $i$, one arrives at the quantity $C(r)$, which is the integral correlation function of the attractor. The nonvanishing of $C(r)$ measures the extent to which the presence of a data point $\mathbf{V}_i$ affects the position of the other points. One shows that for small $r$, $C(r) \sim r^{\nu}$, and the correlation dimension $\nu$ of the attractor is therefore given by the slope of log $C(r)$ versus log $r$.

With the help of this last relation, the dimension $\nu$ is computed by considering successively higher embedding dimensions $p$ of the phase space. If the $\nu$ versus $p$ dependence is saturated beyond some relatively small $p$, the system represented by the time series should possess an attractor. The saturation value $\nu_e$ is regarded as the dimensionality of the attractor of the system represented by the time series. The value of $p$ beyond which saturation is observed provides the minimum number of variables necessary to model the dynamics of the attractor.

The slope of the curve log $C(r)$ versus log $r$ (Fig. 4) has been evaluated with extreme care. After determining the boundaries of the linear zone by visual inspection, we determine the slope of $m$ first points in this segment by the least-squares method. The operation is repeated all along the linear region by sliding $m$ one point further. The computation is repeated for increasing values of $m$. If the region is linear, all these operations must yield the same value of the slope (within acceptable error boundaries).

Although in principle every value of time lag $\tau$ is acceptable for the resurrection of the system's dynamics, in practice, for a given time series, only a well-defined range of $\tau$ (here, $17\ \Delta t \leq \tau \leq 25\ \Delta t$) gives satisfactory linear regions or well-behaved saturation curves.

Fig. 5 shows a saturation curve computed from the epileptic signal. For comparison, the behavior obtained from a random process such as gaussian white noise is drawn. We find a satisfactory saturation beyond the embedding dimension five, which yields a correlation dimension $\nu_e = 2.05 \pm 0.09$. Such a low dimension chaos in a biological system as complex as the brain is striking. It shows the extreme coherence of the dynamical activity recorded by the EEG during the seizure.

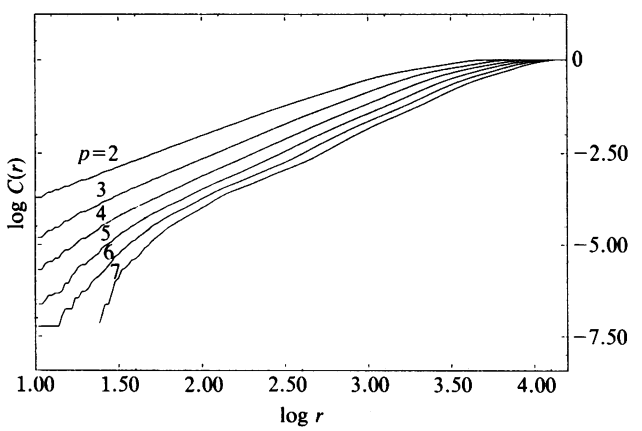


FIG. 4. Dependence of the integral correlation function $C(r)$ on the distance $r$ ($n = 6000$, $\tau = 19\ \Delta t$).

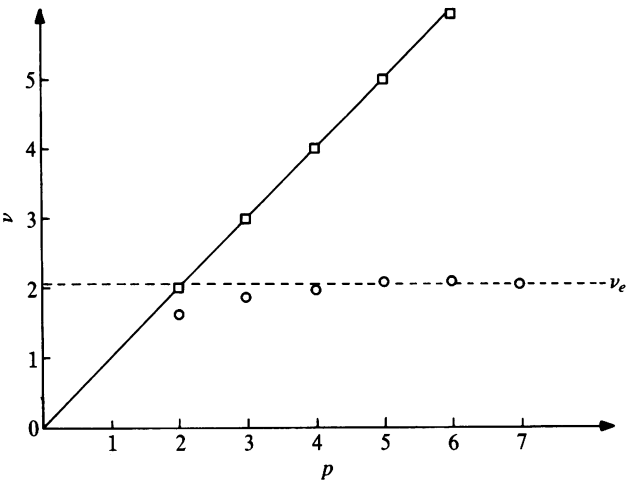


FIG. 5. Dependence of the correlation dimension $\nu$ on the embedding dimension $p$ for a white noise signal (□) and for the epileptic attractor (○) with $\tau = 19\ \Delta t$. The saturation toward a value $\nu_e$ is the manifestation of a deterministic dynamics.

## Time-Dependent Properties

The fundamental unpredictability inherent in a chaotic attractor may be seen by evaluating the normalized time autocorrelation function of the variable $V$:

$$\psi(\tau) = \frac{\frac{1}{N}\sum_{i=1}^{N}[V(t_i) - \overline{V}][V(t_i + \tau) - \overline{V}]}{\frac{1}{N}\sum_{i=1}^{N}[V(t_i - \overline{V}]^2},$$

where

$$\overline{V} = \frac{1}{N}\sum_{i=1}^{N} V(t_i).$$

$\psi(\tau)$ is a measure of the relationship between the value of $V$ at two different instants separated by $\tau$ seconds and averaged over the total length of the series. The sooner $\psi$ vanishes, the more unpredictable is the original signal. For example, the autocorrelation function of a white noise is a $\delta$ function indicating a complete unpredictability, whereas the autocorrelation function of a periodic motion shows sustained periodic oscillations.

Fig. 6*a* depicts the time autocorrelation function evaluated from the time series of Fig. 1 showing irregular damped oscillations. The damping of oscillations indicates the memory loss in the signal that is characteristic of chaotic or stochastic dynamics. Fig. 6*b* shows, in logarithmic scale, the power spectrum of the same signal.

Although in the presence of a chaotic attractor all trajectories converge toward a subset of the phase space, inside the attractor, two neighboring trajectories may diverge. This fact reflects the extreme sensitivity of chaotic dynamics to the initial conditions. The rate of the divergence of the trajectories in time may be assessed from a time series (13). The Lyapunov exponents $\lambda_i$ are the average of these individual evaluations over a large number of trials. A negative Lyapunov exponent indicates an exponential approach of the initial conditions on the attractor; on the contrary, a positive $\lambda_i$ expresses the exponential divergence on an otherwise stable attractor. Thus, a positive Lyapunov exponent indicates the presence of chaotic dynamics.

Using the Fortran code described in ref. 13, we evaluated the largest positive Lyapunov exponent $\lambda$ for an epileptic

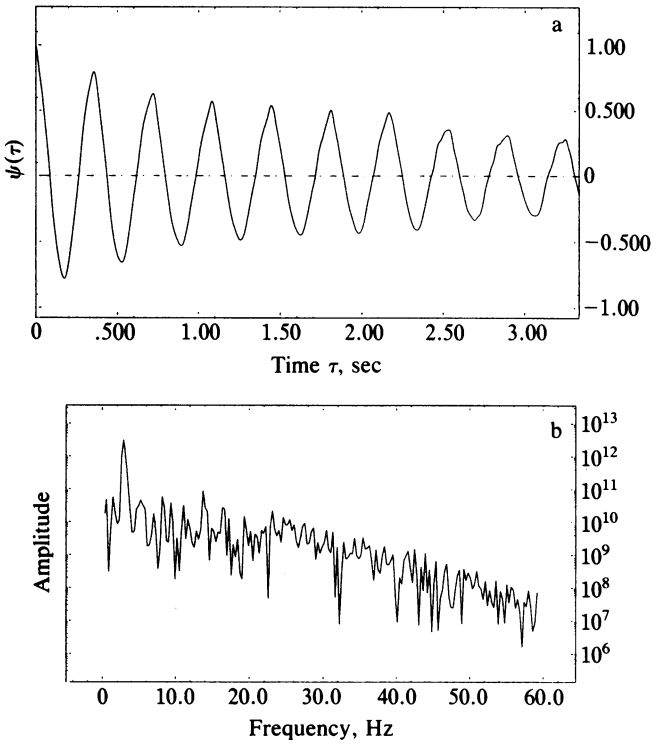


FIG. 6. (*a*) Normalized time autocorrelation function $\psi(\tau)$ of the epileptic signal computed from the first channel of Fig. 1. This function measures the mean similarity of the signal with itself after a time $\tau$. The exponential decay of this value shows a loss of memory and confirms the presence of chaotic dynamics. (*b*) The broad-band nature of the power spectrum is another aspect of chaotic systems. We see the prominent peak in ≈3 Hz.

seizure by examining the divergence of two neighboring trajectories on the attractor. Let us consider the initial point $V(t_0)$ on the phase space and another point on a close by trajectory. $L(t_0)$ is the distance between these two points. The pair of points is allowed to evolve on their respective trajectories for time $t_e$. Now the distance between the two trajectories is $L(t_1)$, where $t_1 = t_0 + t_e$. The largest Lyapunov exponent is given by

$$\lambda = [1/t_e][\log_2 L(t_1) - \log_2 L(t_0)].$$

Another point in the neighborhood of $V(t_0)$ is chosen and the procedure is repeated until all points in the time series are scanned. This procedure must converge to a constant value of the exponent $\lambda$. The choice of the neighboring trajectory is not easy and is sensitive to the internal structure of the attractor; satisfactory results are found only in a narrow range of parameters. Moreover, all values of $\lambda$ must converge toward a unique limit as $t_e$ is increased. Fig. 7 shows three trials out of a total of nine that were necessary to estimate the correct value of $\lambda$. We find a positive value of the order of $\lambda = 2.9 \pm 0.6$. The inverse of this quantity gives the limit of predictability of the long-term behavior of the system. This time (≈0.35 sec) must be compared with the approximate pseudocycle of 0.35 sec of epileptic phenomena. Thus, there is a gradual loss of memory after each pseudocycle.

### Normal Brain Activity

The EEG data recorded from the human brain during sleep cycles were also analyzed according to the procedure cited above (7). Chaotic attractors were identified for stage two and stage four of deep sleep. These attractors were characterized by a rather low dimensionality, which decreases as

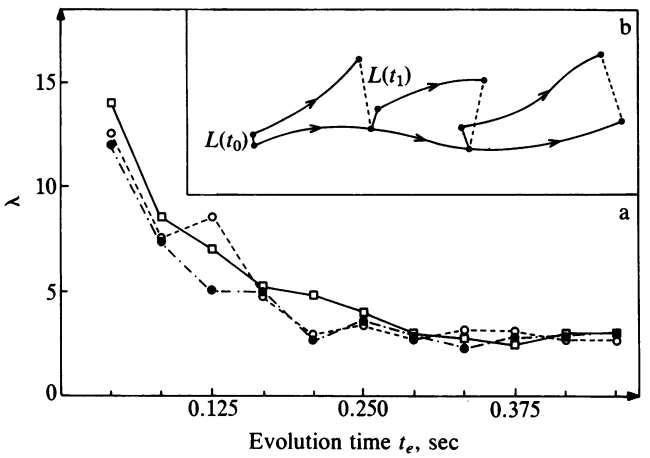


FIG. 7. (*a*) The greatest Lyapunov exponent $\lambda$ as a function of $t_e$ for $n = 6000$ points, $p = 5$, and $\tau = 20\ \Delta t$. Three trials are shown for various estimates of the local structure of the attractor. A lower bound of 5% and upper bounds of 10% (□), 15% (○), and 20% (●) of the spatial extent of the attractor were considered. (*b*) Schematic representation of the procedure.

the sleep cycle unfolds. The most coherent dynamics stems for deep sleep stage four. Fig. 8 shows the phase space portrait of the attractor, with $\nu_s = 4.05 \pm 0.05$.

Preliminary studies did not reveal, in a space of relatively low embedding dimension ($p \leq 10$), the presence of chaotic attractors during the awake stage (alpha waves) and the rapid eye movement stages of sleep. Table 1 shows the embedding dimension and the fractal dimension of various stages of brain activity compared with three variable attractors of Lorenz and Rössler models (10–14). We see a big jump in the dimensionality and, therefore, in the coherence of the underlying dynamics, between sleep stage four and the epileptic attractor.

### Conclusions

We have shown that from a routine EEG recording, the dynamics of brain activity could be reconstructed. The fact

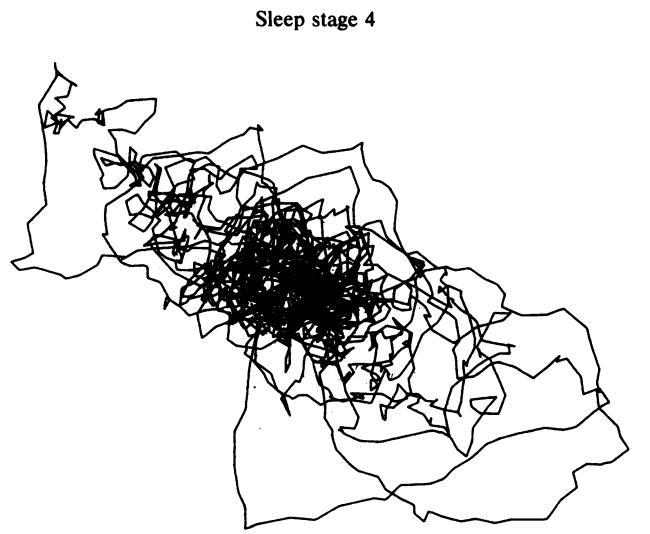


FIG. 8. Phase portrait of EEG recorded from human sleep stage four following a procedure identical to that used in Fig. 2 ($n = 2000$ equidistant points sampled at 100 Hz and $\tau = 10\ \Delta t$).

Table 1. Dimensionality of brain attractors

| Stages of brain dynamics | Embedding dimension $p$ | Attractor dimension $\nu$ |
|---|---|---|
| Awake | $p > 9$ | No saturation |
| Sleep 2 | 6 | 5.03 ± 0.07 |
| | | 5.0 ± 0.1 |
| Sleep 4 | 5 | 4.05 ± 0.05 |
| | | 4.08 ± 0.05 |
| | | 4.4 ± 0.1 |
| REM | $p > 9$ | No saturation |
| Epilepsy | 5 | 2.05 ± 0.09 |
| Lorenz | 3 | 2.05 ± 0.01 |
| Rössler | 3 | 2.01 ± 0.01 |

Embedding dimension of the phase space and correlation dimension of the attractors for various stages of brain dynamics. Each value of $\nu$ corresponds to the EEG activity of a different subject. The Lorenz and Rössler attractors are shown in comparison. REM, rapid eye movement.

that chaotic attractors could be identified for several stages of normal and pathological brain activity indicates the presence of deterministic dynamics of a complex nature. This property should be related to the ability of the brain to generate and process information.

The low value of 2.05 for an episode of petit mal is striking, especially when it is contrasted with the values of 2.2–3.5 found for single neuron recordings from normal monkeys (15). In single neurons, the pseudocycles are of the order of 17–32 msec, whereas in the case of a seizure, we are dealing with cooperative phenomena of the order of 300 msec involving the entire cerebral cortex.

Unlike periodic phenomena, which are characterized by a limited number of frequencies, chaotic dynamics show a broad-band spectrum. Thus, chaotic dynamics increase the resonance capacity of the brain. In other words, although globally a chaotic attractor shows asymptotic stability, there is an internal instability reflected by the presence of positive Lyapunov exponents. This results in a great sensitivity to the initial conditions and, thus, an extremely rich response to external input.

In the light of such concepts, we may speculate further and suggest the following explanation for the type of petit mal epileptic seizure studied in this paper: the agents producing the seizure tend to drive the brain activity toward a stable periodic motion. In such states, information processing would be impossible and recovery would be extremely difficult. However, the brain manages to remain on a chaotic attractor, although one of a very low dimensionality, in order to process reflex activities.

The topological properties of the attractors and their quantification by means of dimensionality analysis may be an appropriate tool in the classification of brain activity and, thus, a possible diagnostic tool. For example, various forms of epileptic seizures could be classified according to their degree of coherence.

The determination of the minimum number of variables necessary for the description of epileptic attractors is a valuable clue for model construction. From our analysis of the epileptic attractor, we may suggest that at least five distinct variables are involved in the onset of petit mal. For example, two variables—the membrane potential of excitatory and inhibitory neurons—have the tendency to generate a periodic behavior, whereas three other variables pull back the attractor into a less coherent state. A model for epileptic seizure based on interaction of a group of excitatory and inhibitory neurons was shown to exhibit biphasic oscillations (16, 17). The model reported in ref. 17 based on interaction of one inhibitory and one excitatory cell was analyzed by using the range of parameters described in refs. 16 and 17. It was found that the differential delay equations describing the model show a stable homogeneous steady state for the delay $t' = 0.01$. However, for $t' = 0.1$, the periodic behavior sets in and is followed by a quasi-periodic behavior for $t' = 0.13$. For larger values of $t'$, the motion becomes chaotic.

We thank I. Prigogine, C. Nicolis, G. Nicolis, M. Salazar, and P. Gaspard for stimulating discussions. G. Engelen is acknowledged for providing some of the computer programs. We are grateful to G. Depiesse, J. Hildebrand, B. Lacroix, J. Mendlewicz, G. Noel, G. Rousseau, J. Shoentgen, and E. Stanus for the recording and transfer of data.

1. Brandstater, A., Swift, J., Swinney, H. L. & Wolf, A. (1983) *Phys. Rev. Lett.* **51**, 1442–1445.
2. Roux, J. C., Simoyi, R. M. & Swinney, H. L. (1983) *Physica D* **8**, 257–266.
3. Nicolis, C. & Nicolis, G. (1984) *Nature (London)* **311**, 529–532.
4. Nicolis, C. & Nicolis, G. (1986) *Proc. Natl. Acad. Sci. USA* **83**, 536–540.
5. Markus, M., Kuschmitz, D. & Hess, B. (1984) *FEBS Lett.* **172**, 235–238.
6. Markus, M., Kuschmitz, D. & Hess, B. (1985) *Biophys. Chem.* **22**, 95–105.
7. Babloyantz, A., Nicolis, C. & Salazar, M. (1985) *Phys. Lett. A* **3**, 152–156.
8. Takens, F. (1981) in *Dynamical Systems and Turbulence, Warwick 1980*, Lecture Notes in Mathematics, eds. Rand, D. A. & Young, L. S. (Springer, Berlin), Vol. 898, pp. 366–381.
9. Leary, J. O. & Goldring, S. (1976) in *Science and Epilepsy* (Raven, New York).
10. Rössler, D. E. (1979) *Ann. N. Y. Acad. Sci.* **316**, 376–392.
11. Grassberger, P. & Procaccia, I. (1983) *Phys. Rev. Lett.* **50**, 346–349.
12. Grassberger, P. & Procaccia, I. (1983) *Physica D* **9**, 189–208.
13. Wolf, A., Swift, J. B., Swinney, H. L. & Vastano, J. A. (1985) *Physica D* **16**, 285–317.
14. Lorenz, E. N. (1963) *J. Atmos. Sci.* **20**, 130–141.
15. Rapp, P. E., Zimmerman, I. D., Albano, A. M., Deguzman, G. C. & Greenbaun, N. N. (1985) *Phys. Lett. A* **110**, 335–338.
16. Kaczmarek, L. K. (1976) *Biol. Cybern.* **22**, 229–234.
17. Babloyantz, A. & Kaczmarek, L. K. (1977) *Biol. Cybern.* **26**, 199–208.